Available online at www.sciencedirect.com
ScienceDirect
European Journal of Medicinal Chemistry 43 (2008) 2549–2556
EUROPEAN JOURNAL OF MEDICINAL CHEMISTRY
http://www.elsevier.com/locate/ejmech

Original article

Synthesis, chemical and biological studies on new Fe^{3+}-glycosilated β-diketo complexes for the treatment of iron deficiency

Beatrice Arezzini [a], Marco Ferrali [a], Erika Ferrari [a], Chiara Frassineti [c], Sandra Lazzari [b], Gaetano Marverti [a], Ferdinando Spagnolo [b], Monica Saladini [b,*]

[a] Department of Physiopathology and Experimental Medicine, University of Siena, Via Aldo Moro 53100 Siena, Italy
[b] Department of Chemistry, University of Modena and Reggio Emilia, Via Campi 183, 41100 Modena, Italy
[c] Department of Biomedical Science, University of Modena and Reggio Emilia, Via Campi 287, 41100 Modena, Italy

Received 4 October 2007; received in revised form 25 February 2008; accepted 29 February 2008
Available online 14 March 2008

Abstract

A simple synthetic pathway to obtain glycosilated β-diketo derivatives is proposed. These compounds show a good iron(III) affinity therefore we may suggest the use of their Fe^{3+}-complexes as oral iron supplements in the treatment of anaemia. The glycosilated compounds (6-GlcH, 6-GlcOH and 6-GlcOCH$_3$) are characterized by means of spectroscopic (UV, ^{1}H and ^{13}C NMR) and potentiometric techniques; they have a good water solubility, are kinetically stable in physiological condition ($t_{1/2} > 100$ h) and show a low cytotoxicity also in high concentrations ($IC_{50} > 400$ μM). They are able to bind Fe^{3+} ion in acid condition (pH ∼ 2) forming complex species thermodynamically more stable than those of other ligands commonly used in the treatment of iron deficiency. The iron complexes show also a good kinetic stability both in acidic and physiological pH and have a good lypophilicity ($\log P > -0.7$) that suggests an efficient gastrointestinal absorption in view of their possible use in oral therapy. In addition they demonstrate a poor affinity for competitive biological metal ion such as Ca^{2+}, and in particular 6-GlcOCH$_3$ is able to inhibit lipid peroxidation.

Keywords: Iron complexes; β-Diketo ligands; Curcumin; Kinetic study; Thermodynamic study; Cytotoxicity

1. Introduction

Iron plays an important role in the living systems, therefore iron deficiency causes anaemia and other pathological changes in the body. In order to prevent and treat this disease some iron containing medicines are used. The advantages and disadvantages of the various preparates are related to the root of administration [1–3]. Under normal circumstances orally administrated iron is the treatment of choice since it is simple, effective, safe and cheap. Actually different iron supplements containing Fe^{2+} or Fe^{3+} complexes or salts (Iron Complex®, Ferro-grad®) are in use. However, oral Fe administration causes various malaises such as nausea, vomiting, pain, diarrhoea and constipation, resulting in poor compliance [4,5]. In case of inadequate gastrointestinal iron absorption or intolerance to the requisite dose of oral iron a parenteral therapy is preferred [6]. Parenteral iron formulations containing iron–sucrose complexes are widely used (Venofer®, Ferrlecit®). A parenteral iron preparation must have a complex ability sufficient to avoid excessive blood concentration of Fe and low toxicity to avoid side effects [7]. Parenteral iron administration is mainly used in treatment of anaemia, in chronic haemodialysis patients and in serious iron deficiency such as in the last month of pregnancy. Great interest is turned on the development of new safe and low toxic iron carriers both for oral and intravenous administration.

Previously we have explored the ability of natural occurring molecules such as curcumin (Scheme 1) and its derivatives to chelate Fe^{3+} ion [8]; the β-diketo moiety of curcumin demonstrated coordination ability toward this metal ion. Its main

* Corresponding author. Tel.: +39 0592055040; fax: +39 059373543.
E-mail address: monica.saladini@unimore.it (M. Saladini).

0223-5234/$ - see front matter © 2008 Elsevier Masson SAS. All rights reserved.
doi:10.1016/j.ejmech.2008.02.045

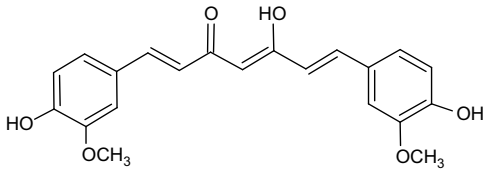

Scheme 1. Curcumin.

drawback in the clinical use is its low water solubility; to overcome this handicap we have synthesized glycosylated curcuminoids [9]. These compounds add iron chelating ability to good water solubility and free-radical scavenging activity, inhibiting the iron redox cycle. In order to reduce molecular weight and favour diffusion through cell membranes, we have also synthesized new glycolsilated compounds derived from curcumin (Scheme 2). For one of them (6-GlcOCH$_3$), a preliminary study on its iron chelating properties has been previously explored [10]. Before proposing these complexes for clinical use as iron supplements in oral therapy, a complete characterization of complexes and ligands have to be done to assure their safety.

In this paper we report a new simplified synthetic pathway with enhanced yield and reduced reaction time for compounds showed in Scheme 2. The effect of the aromatic ring substituents on iron complexes' stability is evaluated together with the affinity toward other physiological metal ions such as Ca^{2+} which may compete with iron in the body. Lipophilicity is an important factor that influences drug absorption by gastrointestinal tract, anyway the chemical stability of the metal carrier in physiological conditions is not less important; so both these aspects are investigated here.

In order to evaluate a possible cytotoxicity of these compounds against normal tissues as a prediction of side effects, we have tested the molecules on the growth of Vero cells. The Vero cell line, an immortal, non-tumorigenic fibroblastic cell line established from kidney cells of the African green monkey (*Cercopithecus aethiops*), has a characteristic growth pattern in culture [11], and has been used to study cell growth, differentiation [12,13], and cytotoxicity [14]. These cells are recommended for such investigations in standard protocols [15] and provide an excellent model for studying alterations in cell growth induced by chemicals *in vitro* because of their characteristic growth pattern and behaviour in culture.

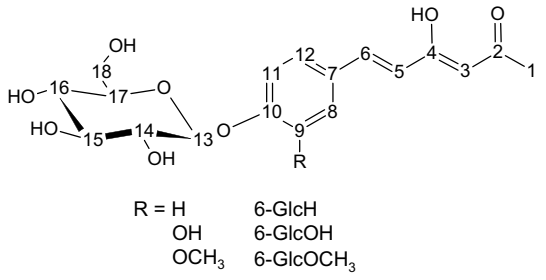

Scheme 2. Synthesised compounds.

2. Experimental section

2.1. Synthesis

2.1.1. 2,3,4,6-Tetracetyl-α-D-glucopyranosyl bromide (*1*)

Compound **1** was synthesized quantitatively by reaction of 1,2,3,4,6-pentaacetyl-β-D-glucopyranose with HBr 30% in glacial acetic acid, at room temperature for 4 h [16].

2.1.2. 4-[(2,3,4,6-Tetracetyl-β-D-glucopyranoside) oxy]benzaldehyde (*2*); 3-hydroxy-4-[(2,3,4,6-tetracetyl-β-D-glucopyranoside)oxy]benzaldehyde (*3*); 3-methoxy-4-[(2,3,4,6-tetracetyl-β-D-glucopyranoside)oxy]-benzaldehyde (*4*)

The appropriate benzaldehyde was solubilized in NaOH, and then slowly dropped in an equimolar solution of **1** in acetone. The reaction was kept under stirring overnight at room temperature, and a precipitate splitted up when water was added. The isolated product was recrystallized from EtOH.

2.1.3. 4-Hydroxy-6-{4-[(2,3,4,6-tetracetyl-β-D-glucopyranoside)oxy]phenyl}hex-3,5-dien-2-one (*5*); 4-hydroxy-6-{3-hydroxy-4-[(2,3,4,6-tetracetyl-β-D-glucopyranoside)oxy]phenyl}hex-3,5-dien-2-one (*6*); 4-hydroxy-6-{3-methoxy-4-[(2,3,4,6-tetracetyl-β-D-glucopyranoside)oxy]phenyl}hex-3,5-dien-2-one (*7*)

A suspension of 4.0×10^{-3} mol of B_2O_3 and 4.0×10^{-3} mol of acetylacetone in DMF (2.0 mL) was stirred for 10 min at 80 °C, followed by the addition of 16.0×10^{-3} mol of tributylborate. After 10 min a solution of 0.8×10^{-3} mol of the appropriate glucosilbenzaldehyde (**2**–**4**) in 1.5 mL of DMF and a solution of 0.8×10^{-3} mol of *n*-butylamine (ButNH$_2$) in 1.5 mL of DMF were slowly dropped (1 h). The solution, kept under stirring at 80 °C for 4 h, developed a yellow-orange colour. The solution was emptied into 15 mL of hot (60 °C) 5% aqueous acetic acid. During the acidification, the solution was cooled to room temperature. The crude product appeared as heavy oil. After about 1 h of stirring, the solvent was removed and the syrup suspended in water at room temperature, as stirring continued, slowly turned into a solid. The crude solid was collected and purified with flash chromatography (silicagel 0.035–0.070 mm; EtOAc/EtPet). *Elemental analysis*: **5** – $C_{26}H_{34}O_{12}$ calcd: C 57.99, H 6.36; experimental: C 58.15, H 6.48; yield 88%; **6** – $C_{26}H_{34}O_{13}$ Calcd: C 56.31, H 6.18; experimental: C 56.15, H 6.50; yield 63%; **7** – $C_{27}H_{36}O_{13}$ calcd: C 57.04, H 6.38; experimental: C 57.60, H 6.45; Yield 42%; NMR chemical shifts (ppm in $CDCl_3$): **5** – H-1 2.16, H-3 5.63, H-5 6.36, H-6 7.50, H-8 7.43, H-9 7.09, H-11 7.09, H-12 7.43; C-1 26.7, C-2 197.4, C-3 100.6, C-4 177.1, C-5 121.6, C-6 138.6, C-7 130.3, C-8 129.2, C-9 116.9, C-10 157.9, C-11 116.9, C-12 129.2; **6** – H-1 2.16, H-3 5.63, H-5 6.34, H-6 7.48, H-8 7.14, H-11 6.96, H-12 7.02; C-1 27.0, C-2 197.9, C-3 101.1, C-4 176.7, C-5 122.5, C-6 138.8, C-7 132.3, C-8 114.6, C-9 147.3, C-10 145.3, C-11 117.1, C-12 120.1; **7** – H-1 2.17, H-3 5.64, H-5 6.36, H-6 7.52, H-8 7.08, H-11 7.04, H-12 7.07; C-1 26.9, C-2 197.7, C-3 101.0, C-4 177.0,

C-5 122.2, C-6 139.1, C-7 131.6, C-8 119.7, C-9 150.9, C-10 147.6, C-11 121.3, C-12 111.6, C–R 56.1.

*2.1.4. 4-Hydroxy-6-{4-[(β-D-glucopyranoside) oxy]phenyl}hex-3,5-dien-2-one (6-GlcH) (**8**); 4-hydroxy-6-{3-hydroxy-4-[β-D-glucopyranoside)oxy]phenyl}hex-3, 5-dien-2-one (6-GlcOH) (**9**); 4-hydroxy-6-{3-methoxy-4-[(β-D-glucopyranoside)oxy]phenyl}hex-3,5-dien-2-one (6-GlcOCH$_3$) (**10**)*

The acetylated compounds, solubilized in methanolic 0.1 M solution of CH_3ONa, were kept under stirring for 2 h; pH was brought to neutrality by use of a DOWEX ion exchange resin, which was finally filtered off, and solutions were evaporated under *vacuum*. The reaction is quantitative. *Elemental analysis*: **8** – $C_{18}H_{22}O_8$ calcd: C 59.01, H 6.05; experimental: C 58.96, H 5.89; **9** – $C_{18}H_{22}O_9$ calcd: C 56.54, H 5.80; experimental: C 56.40, H 5.40; **10** – $C_{19}H_{24}O_9$ calcd: C 57.57, H 6.10; experimental: C 57.43, H 6.37.

2.2. Spectroscopy

Spectrophotometric titrations were performed using Jasco V-570 spectrophotometer at 25.0 ± 0.1 °C in the 200–600 nm spectral range employing a 1 cm quartz cell. 2.5×10^{-5} M aqueous solutions of ligands were investigated varying the pH value by adding small amounts of concentrated NaOH or HCl in the pH range 1–11. The protonation constants of the ligands were evaluated from spectrophotometric titrations using the pHab2000 software [17]. Constant additions (10 μL each time) of Fe^{3+} solution (10^{-2} M) were performed using a micropipette in order to reach different M/L molar ratios.

The chemical stability of the ligands was evaluated as a change in absorbance at 345 nm. The ligands solutions of 5×10^{-5} M were prepared in 10^{-2} M phosphate-buffered solution (pH 7). The ligands stability was investigated also in presence of Fe^{3+} in M/L 1:1 molar ratio at pH 2 (HCl 0.01 M) and pH 7 (NaH_2PO_4/Na_2HPO_4). A constant ionic strength of 0.1 M ($NaNO_3$) was maintained in all experiments. The cell was stored at 37 °C in the dark.

NMR spectra were recorded on a Bruker Avance AMX-400 spectrometer with a Broad Band 5 mm probe (inverse detection). Nominal frequencies are 100.13 MHz for ^{13}C and 400.13 MHz for ^{1}H. The typical acquisition parameters for ^{1}H are as follows: 20 ppm spectral bandwidth (SW), 6.1 μs pulse width (90° pulse hard pulse on ^{1}H), 0.5–1 s pulse delay, 216–512 number of scans. For each ligand 0.5 mL of a 10^{-2} M solution was prepared in CD_3OD, then 10 additions (10 μL each time) of $Ga(NO_3)_3$ or $CaCl_2$ solution (5×10^{-2} M in CD_3OD) were performed using a micropipette.

2.3. Potentiometry

Potentiometric measurements were performed in aqueous solution at 25.0 ± 0.1 °C according to general procedures previously reported [18]. A constant ionic strength of 0.1 M (solid $NaNO_3$) and nitrogen gas was maintained in all experiments. The stability constants were refined with Hyperquad program [19] taking into account $[Fe(OH)]^{2+}$ and $[Fe(OH)_2]^{+}$ species [20]. The protonation constants of the ligands were determined by titration of 3×10^{-3} M solutions. The Fe^{3+}/ligand and Ca^{2+}/ligand systems were investigated in 1:1, 1:2 and 1:3 molar ratios ($[Fe^{3+}]$ and $[Ca^{2+}]$ ranges 3×10^{-3}–1×10^{-3} M). Aqueous NaOH (1×10^{-2} M) was used as titrant. A measuring time of 600–720 s for each point was used. At least 10 measurements were performed for each system with 40 data points in each titration in the pH range 2–10.

2.4. Partition coefficient

The shake-flask method was performed on each ligand and on the M/L 1:3 system at pH 7.0 (NaH_2PO_4/Na_2HPO_4). With a known volume of water (15–30 mL) previously saturated with high purity analytical grade *n*-octanol, 25 mL of the ligand stock solution (10^{-4} M) or M/L 1:3 solution (10^{-4} M) were mixed in a vessel and then shaken at 37 °C for 4 h. After separation of the two phases, the ligand concentration in aqueous solution was determined by spectrophotometric method using a Jasco V-570 spectrophotometer.

2.5. Cytotoxicity assays

Vero cells, obtained from the ''Istituto Zooprofilattico'' (Brescia, Italy), were maintained in MEM medium (Whittaker Bioproducts, Walkersville, MD, USA) supplemented with 10% heat-inactivated fetal calf serum (Gibco/BRL, Gaithersburg, MD, USA) and penicillin G (100 μg/mL), streptomycin (100 μg/mL) (Sigma Chemical Company, MO, USA). Cultures were equilibrated with humidified 5% CO_2 in air at 37 °C. The medium was renewed at 48 h intervals, and the cells were always subcultured when the monolayers become confluent.

The cytotoxicity of compounds 6-GlcH, 6-GlcOH, 6-GlcOCH$_3$ and Curcumin on Vero cells was assessed by a modification of the crystal violet dye assay [21]. In this protocol, Vero cells were seeded at a density of 4×10^4 cells/well of a 24-well culture plate (Sarstedt, Numbrecht, Germany) and cultured for 72 h at 37 °C (control cells). Treated cells were incubated with different concentrations of the compounds and were grown under the same conditions as non-treated (control) cells. After incubation, the culture medium was removed and the cells were washed with 0.1 mL of 0.1 M phosphate-buffered saline (PBS), pH 7.4 at 37 °C, then cell monolayer was fixed with methanol prior to staining with 0.25% crystal violet solution in 80% absolute ethanol for at least 30 min. After washing several times with distilled water to remove the excess dye, the cells were let to dry. The incorporated dye was solubilized in acidic isopropanol (1 N HCl/2-propanol, 1:10). After appropriate dilution, dye was determined spectrophotometrically at 540 nm. The extracted dye was proportional to cell number. Percentage of survival was calculated by comparing the absorbances of exposed to that of non-exposed (control) cultures.

Rat liver microsomes were prepared in Tris–maleate buffer (pH 7.4) following a standard procedure and resuspended in the same buffer at the concentration of 2.5 mg protein/mL

Table 1
^{1}H chemical shifts (δ ppm) of ligands, their gallium(III) complexes and $\Delta\delta$ ($\delta_{complex} - \delta_{ligand}$) registered at 300 K in CD_3OD

	H-1	H-3	H-5	H-6	H-8	H-9	H-11	H-12	H–R
6-GlcH	2.17	5.82	6.57	7.58	7.58	7.15	7.15	7.58	–
M/L 1:3	2.21 (0.04)	5.91 (0.09)	6.72 (0.15)	7.79 (0.21)	7.63 (0.05)	7.16 (0.01)	7.16 (0.01)	7.63 (0.05)	–
M/L 1:1	2.25 (0.08)	[a]	6.76 (0.19)	7.86 (0.28)	7.65 (0.07)	7.17 (0.02)	7.17 (0.02)	7.65 (0.07)	–
6-GlcOH	2.17	5.81	6.51	7.51	7.14		7.23	7.07	–
M/L 1:3	2.21 (0.04)	[a]	6.67 (0.16)	7.72 (0.21)	7.18 (0.04)		7.25 (0.02)	7.11 (0.04)	–
M/L 1:1	2.25 (0.08)	[a]	6.70 (0.19)	7.79 (0.28)	7.20 (0.06)		7.26 (0.03)	7.14 (0.07)	–
6-GlcOCH$_3$	2.10	5.83	6.59	7.57	7.20		7.20	7.29	3.94
M/L 1:3	2.19 (0.09)	5.90 (0.07)	6.73 (0.14)	7.75 (0.18)	7.30 (0.10)		7.20 (0.00)	7.20 (0.09)	3.92 (0.02)
M/L 1:1	2.24 (0.14)	6.00 (0.17)	6.77 (0.18)	7.82 (0.25)	7.31 (0.11)		7.21 (0.01)	7.21 (0.08)	3.92 (0.02)

[a] The methylenic proton is mobile, in fast exchange with residual HOD.

[9]. Microsomal membranes were incubated at 37 °C at the concentration of 1.25 mg/mL of protein in the presence of 100 μM Fe^{3+}–2.5 mM ADP and different concentrations of the complexants (100–300 μM) dissolved in small volumes of ethanol. Samples of the mixture were withdrawn at the indicated times and the lipid peroxidation measured with a standard procedure [9].

3. Results and discussion

3.1. NMR spectroscopy

Ligand molecules show a typical spectrum of a β-keto-enolic moiety [9,22], the enolic proton is mobile, in fast exchange with residual HOD and implied in a strong intra-molecular hydrogen bond, as confirmed by crystal structure of analogous compounds [23], that makes it equally shared by the two oxygen atoms. NMR signal of enolic proton is a very broad peak around 16–17 ppm, depending on the substituent.

$Ga(NO_3)_3$ is used as NMR probe instead of Fe^{3+}; its addition to the ligand solution, at acidic pH, immediately originates a complex species, in slow chemical exchange in NMR time scale, whose spectral pattern resembles one of the free ligands but is strongly shifted downfield. The complete formation of this species is reached when M/L is 1:3, with disappearance of the signals of the free ligand. As long as gallium ion is added a new downfielded species appears, hinting the formation of another complex species, characterized by a M/L 1:1 independently on the ligand (Tables 1 and 2). By adding Ca^{2+} to the ligand solution no resonances's shifts are observed, even in high excess of metal ions and increasing pH, suggesting a poor ability to bind Ca^{2+} ion.

3.2. UV–vis spectroscopy

All the compounds are characterised by a maximum of absorbance in the 320–345 nm spectral range with a red shift on increasing pH (340–365 nm). By plotting absorbance vs. pH, one equivalent point is observed corresponding to enolic proton dissociation for all the compounds, while for 6-GlcOH a second equivalent point corresponding to phenolic proton dissociation is found; the pK_a values calculated from spectrophotometric data are reported in Table 3.

By adding Fe^{3+} solution to the free ligands in acidic condition (pH ∼ 4.5) a general increase in absorbance is observed and a new band appears around 400 nm (Fig. 1), due to the interaction of Fe^{3+} with the β-diketo moiety with an anticipated enolic dissociation with respect to the free ligand ($\Delta pK_a \sim 4$). The absorbance rises with M/L molar ratio and reaches a maximum at M/L 1:1 as detected by NMR data.

3.3. Kinetic study

For all the ligands and their Fe/L 1:1 systems, the plotting of $\ln(A_t/A_0)$ versus time gives a linear regression, hinting a first order kinetic process at 37 °C and constant ionic strength. Fig. 2 shows that ligands' degradation process is extremely slow being the percentage of decomposed ligand less than

Table 2
^{13}C chemical shifts (δ ppm) of ligands and their gallium(III) complexes registered at 300 K in CD_3OD

	C-1	C-2	C-3	C-4	C-5	C-6	C-7	C-8	C-9	C-10	C-11	C-12	C–R
6-GlcH	27.3	200.1	102.5	179.3	123.0	141.4	131.6	131.4	118.9	163.1	118.9	131.4	
M/L 1:3	28.4	197.6	103.4	186.1	126.1	144.1	131.3	131.9	119.0	161.8	119.0	131.9	
M/L 1:1	28.5	198.0	103.9	186.4	125.6	145.3	130.9	132.0	118.9	162.0	118.9	132.0	
6-GlcOH	27.8	199.4	102.6	178.4	123.3	141.6	132.9	116.7	149.4	149.5	119.2	122.8	
M/L 1:3	28.1	197.8	103.7	186.0	126.1	144.0	132.5	116.7	149.6	149.6	118.9	123.0	
M/L 1:1	28.4	198.6	104.2	186.6	125.7	145.8	132.3	117.2	149.6	149.6	119.0	123.7	
6-GlcOCH$_3$	27.5	200.0	102.7	178.9	123.1	141.1	132.2	118.3	151.7	150.4	123.9	113.0	57.5
M/L 1:3	28.2	197.4	103.6	186.1	126.2	143.9	131.9	118.1	151.9	150.9	124.5	113.2	57.5
M/L 1:1	28.4	198.3	104.1	186.5	125.2	145.4	131.4	117.8	151.8	151.3	124.8	113.4	57.5

Table 3
Logarithms of protonation constants of the ligands calculated using spectrophotometric and potentiometric data

	6-GlcH			6-GlcOH[a]			6-GlcOCH$_3$		
pK_{a1}	9.26(3) 9.22(5)[b]			8.03(6) 8.03(9)[b]			8.75(2) 8.73(2)[b]		
pK_{a2}				9.44(7) 9.48(6) [b]					
	Fe^{3+}	Ga^{3+}	Ca^{2+}	Fe^{3+}	Ga^{3+}	Ca^{2+}	Fe^{3+}[c]	Ga^{3+}	Ca^{2+}
[ML]	10.22(8)	10.39(7)	2.69(6)	9.5(1)	9.1(1)	1.56(7)	9.71(3)	9.6(2)	2.11(5)
[ML(OH)]	6.77(5)	7.04(5)		4.48(9)	4.98(9)		5.83(4)	6.01(7)	
[ML_2]	18.61(5)	19.23(7)	5.56(9)	18.2(1)	17.8 (1)	5.72(5)	18.7(2)	19.02(5)	5.34(4)
[ML_2(OH)]	12.37(7)	14.77(9)		13.2(1)	13.1(1)		14.2(4)	13.5(5)	
[ML_3]	25.59(8)	27.05(9)		26.0(2)	25.7(2)		27.3(8)	26.8(7)	

Formation constants of complex species are estimated using potentiometric data [$T = 25$ °C, $I = 0.1$ M ($NaNO_3$)].
[a] For 6-GlcOH log K values are evaluated taking into account the overall stability constants and protonation constants of the ligand.
[b] Spectrophotometric data.
[c] Values taken from Ref. [10].

10% after 8 h at pH 7, while curcumin, in similar conditions, is almost completely decomposed after 1 h [24]. The presence of sugar moiety and the reduced conjugation in molecular skeleton of our ligands with respect to curcumin, delays degradation processes by increasing $t_{1/2}$ (>100 h for all our compounds vs. 10 min of curcumin) resembling the stability of cyclodextrin complexed curcumin ($t_{1/2} > 100$) [25]. The kinetic stability of the ligands is also confirmed by NMR data, in fact no relevant changes in ^{1}H chemical shifts and integrated areas are observed in the spectra during the first 72 h. The nature of the substituent doesn't drive the degradation process, although 6-GlcH is the more stable one.

At physiological pH the presence of Fe^{3+} in M/L 1:1 molar ratio seems not to influence the decomposition process, while the same system in acidic condition (pH = 2) revealed a higher stability (degradation after 8 h < 5%).

3.4. Potentiometric titrations

The protonation constants of the ligands were determined both by spectrophotometric and potentiometric methods and the differences range from 0.02 to 0.04 (Table 3). Potentiometric analysis gives more accurate results than other techniques; therefore, we decided to evaluate log K of the complexes only by potentiometry. The substituent on the aromatic ring influences the pK_a value of the ligands; the electron-withdrawing effect of the substituent in *meta* position lowers the pK_a value in the order 6-GlcOH < 6-GlcOCH$_3$ < 6-GlcH.

The species distribution curves of Fe^{3+} complexes of 6-GlcH are reported in Fig. 3, while Table 3 shows logarithms of calculated stability constants. At acidic pH (~2) the prevailing species is [FeL], confirming UV and NMR data. In this complex Fe^{3+} is coordinated by the ligand molecule acting as chelating agent through the dissociated keto-enolic moiety. On increasing pH the complex system may suffer from the competition of OH^- groups till $Fe(OH)_3$ precipitation, as reported in the distribution curves obtained taking into account K_{ps} of $Fe(OH)_3$ [26]; anyway, once iron is uptaken from the gastrointestinal tract, $Fe(OH)_3$ precipitation is prevented by the interaction with specific Fe-proteins deputated to iron homeostasis in biological systems.

A comparison between Fe^{3+}-complexes with our ligands and those with gluconic acid [27], which is the most widely used Fe^{3+}-supplier in treatment of anaemia, is forbidden on the basis of stability constant values due to the different stoichiometry of the formed species. Anyway the amount of free iron at acidic pH (~2) is around 60% for gluconic acid, 20% for 6-GlcOH, 30%

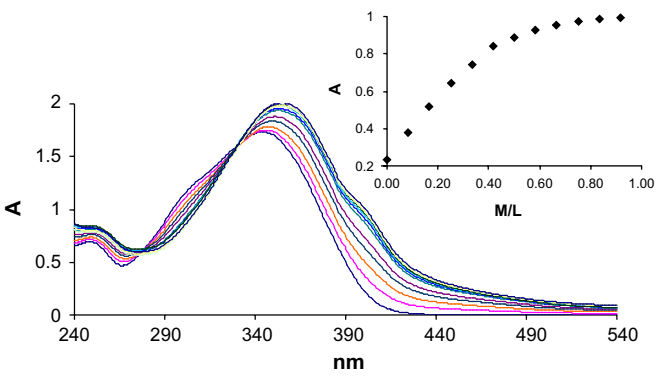

Fig. 1. Spectrophotometric titration of 6-GlcOH solution with $Fe(NO_3)_3$. The inset shows the plot of absorbance vs. M/L molar ratio at $\lambda = 400$ nm.

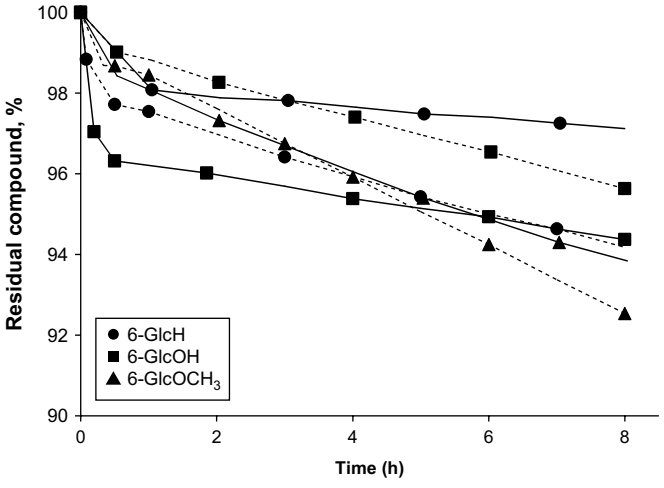

Fig. 2. Plotting of residual compound percentage versus time (h) for all ligands (continuous line) and Fe/L 1:1 systems (broken line). Spectrophotometric measurements were performed in buffer solution (pH = 7) at 37 °C in the dark, $[L]_0 = 2.5 \times 10^{-5}$ M.

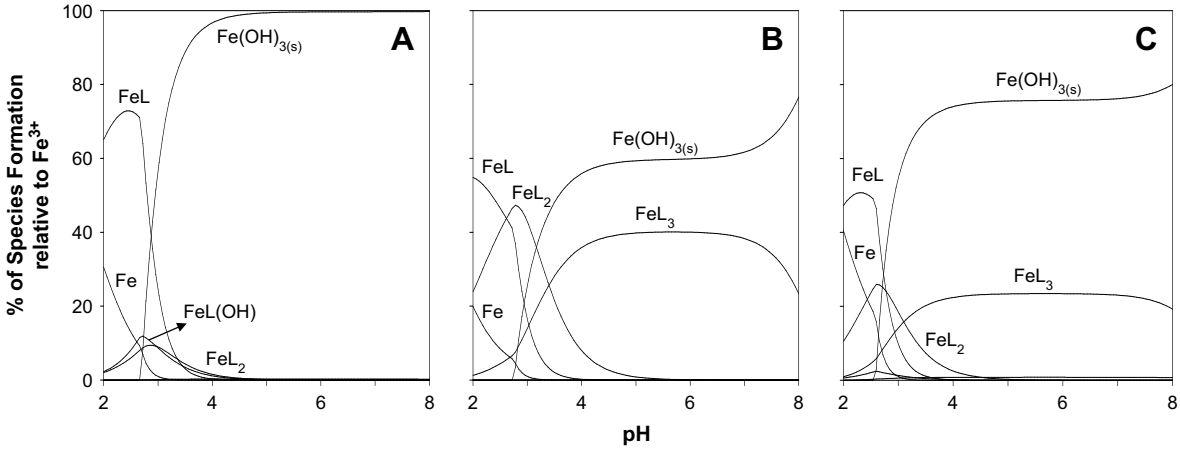

Fig. 3. Species distribution curves of Fe^{3+}/L systems: (A) Fe/6-GlcH; (B) Fe/6-GlcOH and (C) Fe/6-GlcOCH$_3$; $[Fe^{3+}]_{total} = 1 \times 10^{-3}$ M, $[L]_{total} = 2 \times 10^{-3}$ M.

for 6-GlcH and 40% for 6-GlcOCH$_3$ suggesting a higher stability of our complexes with respect to gluconic acid; this feature is fundamental for a good gastrointestinal absorption in view of a potential oral administration.

As Ca^{2+} is one of the most abundant metal ion in human body, being its concentration in physiological fluids about 1.2 mM [28], we have evaluated its possible competition with iron in the interaction with our ligands. Fig. 4 shows the distribution curves of Ca^{2+}/6-GlcOH system with respect to the ligand, calculated using the stability constants reported in Table 3. Up to physiological pH, the affinity of 6-GlcOH for proton is higher than that for calcium, whereas in basic condition (pH ~ 9) only 20% of the ligand is coordinated to calcium ion. This percentage dramatically decreases in presence of iron (Fe/Ca 1:5) confirming the poor affinity for calcium ion as already observed by ^{1}H NMR data.

3.5. Partition coefficients

The efficient penetration through biomembranes is a prerequisite for oral administration of Fe containing drugs; this ability is described by the partition coefficient between *n*-octanol and buffered aqueous solution (pH = 7.0). Table 4 reports the log *P* values for both ligands and complexes. The log *P* value of the ligands is mostly influenced by the nature of the substituent in *meta* position in the aromatic ring: the increased hydrophilic character of OCH_3 with respect to H decreases the log *P* value, while the presence of OH favours the formation of intra-molecular hydrogen bond interactions with the glycosidic moiety diminishing the hydrophilicity of the compound [29]. The lipid solubility of Fe-complexes is lower than that of the corresponding ligand but is sufficient to give an efficient absorption from the gastrointestinal tract ($\log P > -0{,}7$) [30]. A linear relationship is often used to correlate the partition coefficients of the free ligand (L) and iron complex (FeL) [31]:

$$\log P_{FeL} = n \log P_L + k$$

where *n* is the stoichiometry of the complex and *k* is a constant representing the change in hydrophobicity in converting the ligating group of the ligand into the iron coordination sphere of the complex. Our data match this behaviour with a calculated $n = 0.95$ and $k = -0.11$.

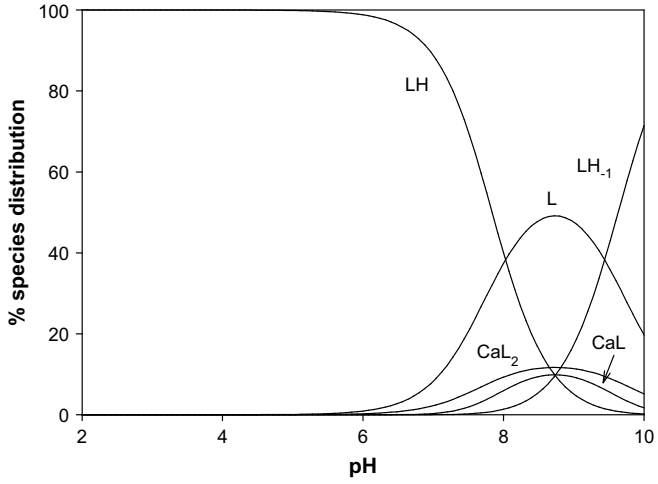

Fig. 4. Species distribution curves for Ca^{2+}/6-GlcOH system; $[Ca^{2+}]_{total} = 1.2 \times 10^{-3}$ M, $[L]_{total} = 7.5 \times 10^{-4}$ M.

3.6. Cytotoxicity

In order to evaluate the possible drawbacks of the free ligands, upon iron delivery, we have tested the inhibitory effect *in vitro* of the compounds against the growth of Vero cells, chosen as control cell line. 6-GlcOH treatment decreases Vero cell proliferation by nearly 10% at 400 μM and by 20% at 800 μM

Table 4
Logarithms of partition coefficient defined as the concentration ratio (mol L^{-1}) in the two solvents (*n*-octanol and water)

	Ligand	Fe–ligand system
6-GlcH	0.39	0.28
6-GlcOH	0.32	0.17
6-GlcOCH$_3$	0.13	0.02

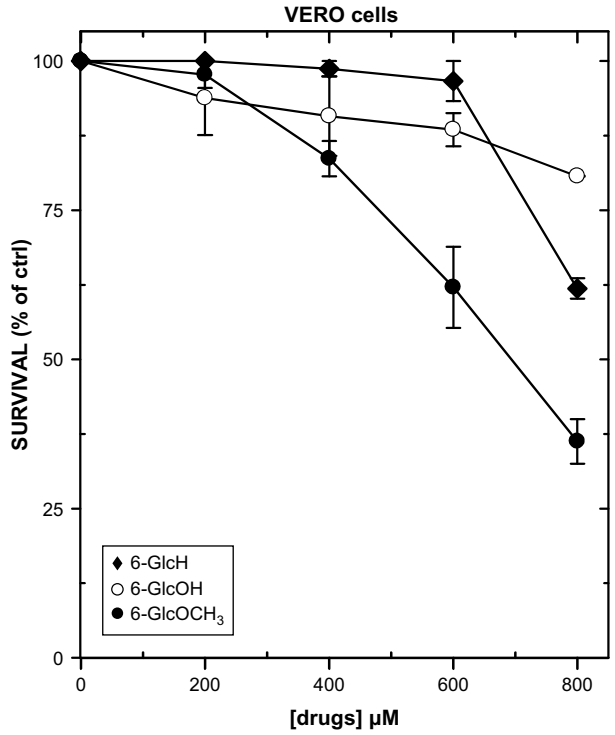

Fig. 5. Survival of VERO cells following treatment with 6-GlcH (◆), 6-GlcOH (○) and 6-GlcOCH$_3$(●). Each point represents mean value ± SD of 3 separate experiments, each conducted with triplicate plates.

(Fig. 5). This inhibition represents an 80-fold lower cytotoxic potency of the compound when compared to curcumin, which shows to inhibit cell growth to the same extent but at greater concentrations (5 and 10 μM for 10% and 20% inibition, respectively). The substitution of OH group with OCH_3 group results in a higher cytotoxicity that is dose-related, since at 600 μM the growth of Vero cells is inhibited by 40% and by 65% at 800 μM, showing an IC_{50} value of nearly 700 μM in the tested drug concentration range. 6-GlcH decreases Vero cell growth by approximately 2% (600 μM) and 40% (800 μM). These results indicate that the three compounds might be well tolerated by normal tissues up to 400 μM, in particular, 6-GlcH seems to be non-toxic up to 600 μM and 6-GlcOH even up to 800 μM. Despite their different behaviour all the compounds show a cytotoxicity extremely lower than curcumin, which is commonly administrated even in high dosages without relevant side effects [32].

Furthermore i*n vitro* experiments to evaluate the effects of iron complexes on subcellular fractions were performed. Rat liver microsomes were incubated with the three compounds, each in the presence of three different Fe^{3+} ratios (Fig. 6). As it can be seen, the presence of 6-GlcH (Fig. 6A) or 6-GlcOH (Fig. 6B), does not attenuate the extent of lipid peroxidation induced by 100 μM Fe^{3+}. When 6-GlcOH is added (Fig. 6B), iron redox activity is even stimulated, indicating a weak bond between iron and the compound which results in a greater redox capability of iron. When 6-GlcOCH$_3$ (Fig. 6C) is present at the 1:3 (Fe:L) ratio, the lipid peroxidation is inhibited within 30 min suggesting that this compound, rather than 6-GlcOH

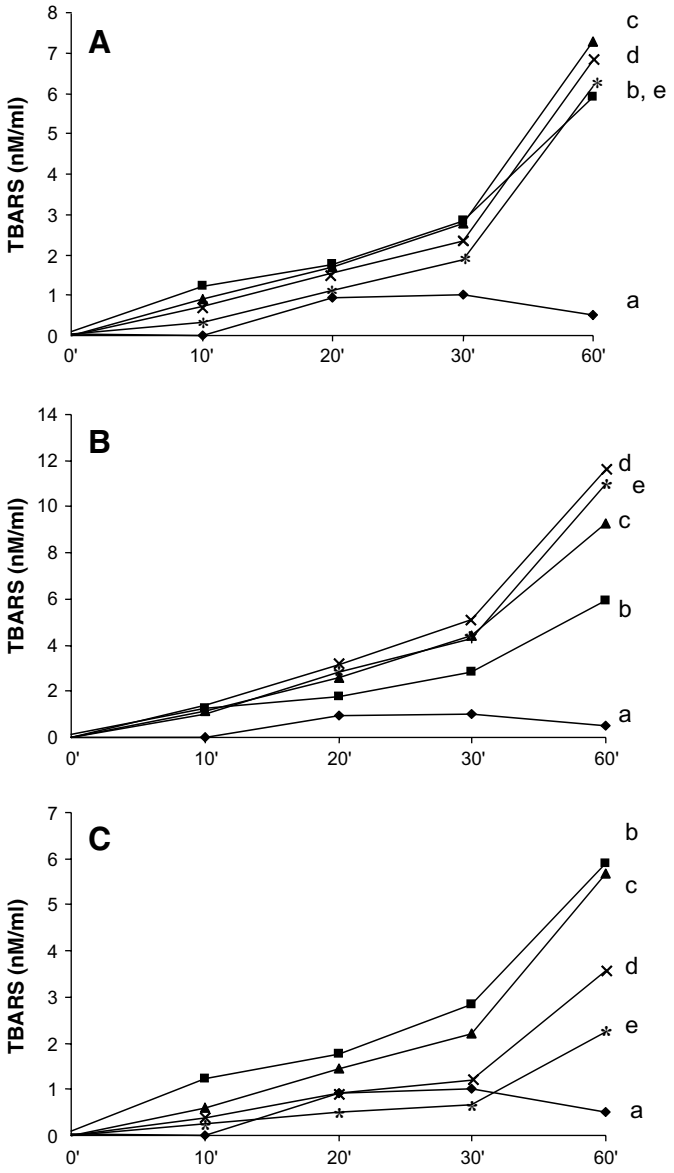

Fig. 6. Time course of thiobarbituric acid reacting substances (TBARS) formation in liver microsomes (MC) incubating at 37 °C in presence of Fe^{3+} and: (A) 6-GlcH; (B) 6-GlcOH; (C) 6-GlcOCH$_3$; (a) —◆— control MC; (b) —■— MC plus 100 μM Fe^{3+}–2.5 mM ADP; (c) —▲— as (b) plus 100 μM chelator; (d) —×— as (b) plus 200 μM chelator; (e) —*— as (b) plus 300 μM chelator. The values represent the mean of two experiments.

or 6-GlcH, is suitable for iron administration as 1:3 complex. Despite the obvious limitations of the *in vitro* observations, these results indicate that 6-GlcOCH$_3$ maintains iron in a redox inactive form before its delivery. On the other hand, its cytotoxicity appears to be relatively low, so that its possible use as iron donor can be worthy of attention.

Acknowledgments

We are grateful to the "Centro Interdipartimentale Grandi Strumenti – C.I.G.S." of the University of Modena and Reggio Emilia and to the "Fondazione Cassa di Risparmio di Modena" for supplying NMR spectrometer.

References

[1] N. Bhandal, R. Russell, BJOG 113 (2006) 1248.
[2] S. Akarsu, E. Taskin, E. Yilmaz, H. Yilmaz, M. Kilic, A.D. Aygun, Acta Haematol. 116 (2006) 51.
[3] A.D. De Silva, E. Tsironi, R.M. Feakins, D.S. Rampton, Alimentary Pharmacol. Ther. 22 (2005) 1097.
[4] L. Hallberg, L. Ryttinger, L. Solvell, Acta Med. Scand. Suppl. 459 (1966) 3.
[5] L. Solvell, Oral iron therapy-side effects, in: L. Hallberg, H.G. Harwerth, A. Vannotti (Eds.), Iron Deficiency: Pathogenesis, Clinical Aspects, Therapy, first ed. Academic Press, London, 1970, pp. 573–583.
[6] O. Schröder, O. Mickisch, U. Seidler, A. de Weerth, A.U. Dignass, H. Herfarth, M. Reinshagen, S. Schreiber, U. Junge, M. Schrott, J. Stein, Am. J. Gastroenterol. 100 (2005) 2503.
[7] G. Perewusnyk, R. Huch, A. Huch, C. Breymann, Brit. J. Nutr. 88 (2002) 3.
[8] M. Borsari, E. Ferrari, R. Grandi, M. Saladini, Inorg. Chim. Acta 328 (2002) 61.
[9] B. Arezzini, M. Ferrali, E. Ferrari, R. Grandi, S. Monti, M. Saladini, Eur. J. Inorg. Chem. 3 (2004) 646.
[10] R. Benassi, E. Ferrari, R. Grandi, S. Lazzari, M. Saladini, J. Inorg. Biochem. 101 (2007) 203.
[11] N.O. Bianchi, J. Ayres, Exp. Cell. Res. 68 (1971) 253.
[12] S.C. Genari, M.A.H. Dolder, M.L.F. Wada, J. Submicrosc. Cytol. Pathol. 28 (1996) 565.
[13] A.R. Santos Jr., H. Dolder, M.L.F. Wada, J. Submicrosc. Cytol. Pathol. 35 (2003) 35.
[14] P. Estacia, A.R. Santos Jr., P.L. Moreira, S.C. Genari, Braz. J. Morphol. Sci. 19 (2002) 41.
[15] ISO 10993-5, Biological Evaluation of Medical Devices Part 5: Tests for Cytoxicity, in vitro Methods, 1992-E.
[16] Fisher, Chem. Ber. (1911) 1898.
[17] P. Gans, A. Sabatini, A. Vacca, Ann. Chim. 89 (1999) 45.
[18] M. Borsari, L. Menabue, M. Saladini, Polyhedron 18 (1999) 1983.
[19] P. Gans, A. Sabatini, A. Vacca, Talanta 43 (1996) 1739.
[20] NIST Standard Reference Database 46, Critically Selected Stability Constants Version 5, <http://webbook.nist.gov>.
[21] W. Kueng, E. Siber, U. Eppenberger, Anal. Biochem. 182 (1989) 16.
[22] E. Solčániova, P. Hrnčiar, T. Liptaj, Org. Magn. Res. 18 (1982) 55.
[23] A.F. Arrieta, A. Mostad, Acta Crystallogr. E57 (2001) o1198.
[24] Y.J. Wang, M.H. Pan, A.L. Cheng, L.I. Lin, Y.S. Ho, C.Y. Hsieh, J.K. Lin, J. Pharm. Biomed. Anal. 15 (1997) 1867.
[25] M.A. Tomren, M. Másson, T. Loftsson, H.H. Tønnensen, Int. J. Pharm. 338 (2007) 27.
[26] X. Liu, F.J. Millero, Geochim. Cosmochim. Acta 63 (1999) 3487.
[27] G.M. Escandar, A.C. Olivieri, M. Gonzalez-Sierra, L.F. Sala, J. Chem. Soc., Dalton Trans. (1994) 1189.
[28] L. Larsson, P. Magnusson, Metal Ions in Biological Systems, vol. 41 (2004) p. 71.
[29] M.D. Habgood, Z.D. Liu, L.S. Dehkordi, H.H. Khodr, J. Abbot, R.C. Hider, Biochem. Pharmacol. 57 (1999) 1305.
[30] Z.D. Liu, R.C. Hider, Med. Res. Rev. 22 (2002) 26.
[31] J.T. Edward, Biometals 11 (1998) 203.
[32] J.J. Johnson, H. Mukhtar, Cancer Lett. 255 (2007) 170.